NtrX systemically controls transcription of the CtrA system genes to regulate *Rhizobium* cell division

Shenghui Xing[#], Fang An[#], Xinwei Yang, Leqi Huang, Shuang Zeng, Ningning Li, Khadidja Ouenzar, Junhui Yan, Liangliang Yu, Li Luo*

Shanghai Key Laboratory of Bio-energy Crops, School of Life Sciences, Shanghai University, Shanghai 200444, China

Running title: NtrX positively controls *Sinorhizobium* cell division

*Correspondence: liluo@shu.edu.cn.

[#]The authors contributed equally to this work.

Abstract

In α-proteobacteria, the CtrA signaling pathway regulates cell cycle progression. A species whose cell duplication is associated with CtrA stability is affected by the response regulator NtrX. However, the function of NtrX acting on the cell cycle

regulation in bacteria remains unclear. Here, we report that NtrX controls transcription of the CtrA system genes involved in cell cycle regulation in a legume symbiont, *Sinorhizobium meliloti*. Three groups of *ntrX* mutants showed the similar cell cycle defects, such as slow growth, abnormal shapes, and irregular genomic DNA accumulation. Expression of the CtrA signaling pathway genes including *ctrA*, *gcrA*, *dnaA*, *divL* and *cpdR1*, is differentially regulated by the phosphorylated NtrX protein. The regulation is achieved through direct protein-DNA interactions. The 53rd aspartate residue known as the conserved phosporylation site and located in the receiver domain of NtrX, is required for *S. meliloti* cell cycle regulation. Interestingly, expression of *S. meliloti ntrX* derivatives in *Caulobacter* and *Agrobacterium* strains showed distinct defects of cell duplication and growth, suggesting that NtrX plays different roles in cell cycle regulation in these bacteria. Our findings demonstrate that NtrX is an upstream transcriptional regulator of the CtrA signaling pathway in *S. meliloti*, which could be associated with nitrogen nutrient response.

Key words:

NtrX; Rhizobium; transcriptional regulation; cell cycle; CtrA

Author Summary

Cell cycle regulation in alpha-proteobacteria is dictated by the conserved CtrA signaling pathway. Transcription of the CtrA system genes is mainly regulated by CtrA and GcrA. CcrM, SciP and MucR also participate in transcription regulation of *ctrA*. However, the regulation by a nutrient response regulator at transcriptional level remains unclear. Here, we report that the nitrogen response regulator, NtrX systemically regulates transcription of several CtrA system genes by protein-DNA interactions in a legume symbiont, *S. meliloti*. The similar mechanism is proposed in the pathogens of *Agrobacterium* and *Brucella* species. These findings provide a new prospect to understand the hierarchy of transcriptional regulation in a bacterial cell cycle.

Introduction

IIn α-proteobacteria, *Caulobacter crescentus* serves as a study model for cell cycle regulation, asymmetric division and cell differentiation. A dividing Caulobacter mother cell produces two daughter cells: a smaller flagellated cell and a larger stalked cell(1). The phosphorylation cascade centered on the response regulator CtrA includes upstream histidine kinases CckA, DivL, DivJ, and PleC, response regulators DivK, ChpT, and CpdR, and transcriptional regulators DnaA, GcrA, SciP, and MucR(1-6). The histidine kinase senses unknown signals, autophosphorylates, sequentially transfers phosphate groups to the response regulator CtrA, and regulates downstream gene (including several transcription factor genes) expression to control flagellar generation, DNA replication, and cell division and differentiation(3).

Unlike *C. crescentus*, rhizobia belonging to α-proteobacteria are usually symbionts of leguminous plants. These bacteria infect specific host legumes under soil nitrogen-limiting conditions, induce nitrogen-fixing root nodule formation, and provide combined nitrogen for host plant growth and development. Rhizobial cell division occurs on the root surface of host plants after adhesion and the inside tubule called an infection thread which extends into root hairs, root epidermal cells and cortical cells, then the bacteria release into the host cytoplasm in the infection zone of legume nodules(7). It has been found that NCR (Nodule Cysteine-Rich) peptides secreted by the host plant determine the terminal differentiation of nitrogen-fixing bacteroids in the indeterminate nodule (such as the root nodules of *Medicago* species)(8-11). However, the regulatory mechanism by which rhizobia duplicate in host cells is largely unknown. Due to the conservation of the CtrA regulatory system in α-proteobacteria, some homologous genes encoding components of this system that function in cell cycle regulation, such as *ctrA*, *ccrM*, *cpdR1*, *divJ*, *divK*, *gcrA*, and *pleC*, have been identified in *Sinorhizobium meliloti* (the symbiont of *Medicago* species)(12-14). Additionally, a few specific genes, such as *cbrA*, are essential for cell cycle regulation through interplay with the CtrA system(15, 16).

The NtrY/NtrX two-component system that was first discovered in *Azorhizobium calinodans*; proved to regulate nitrogen metabolism under free-living conditions, and affect nodulation and nitrogen fixation in the host *Sesbania rostrata*(17). Subsequently, genes homologous to *ntrY*/*ntrX* have been found to regulate nitrogen metabolism and symbiotic nodulation in *Rhizobium tropici*(18). Moreover, the NtrY/NtrX homologous system regulates nitrate uptake in *Azospirillum brasilense* and *Herbaspirillum seropedicae*(19, 20), and this regulatory system has been found to simultaneously control nitrogen metabolism and cellular redox status in *Rhodobacter capsulatus*(21), and to regulate cell envelope formation in *R. sphaeroides*(22). In *Brucella abortus*, the histidine kinase NtrY participates in micro-oxygen signaling and nitrogen respiration (23), and in *Neisseria gonorrhoeae*, the response regulator NtrX controls expression of respiratory enzymes (24). Interestingly, the NtrY/NtrX system regulates cell proliferation, amino acid metabolism and CtrA degradation in *Ehrlichia chaffeensis*(25). NtrX is required for survival of *C. crescentus* cells and its expression is induced by low pH(26). These findings indicated that bacterial NtrY/NtrX comprises a nitrogen metabolism regulatory system that may be associated with cell cycle regulation.

The NtrY component is a transmembrane histidine kinase, and NtrX is a response regulator of the NtrC family, consisting of a DNA-binding domain and a receiver (REC) domain(27, 28). X-ray diffraction crystallography data for the *B. abortus* NtrX protein indicate the following: the protein exists as a dimer; its REC domain is mainly composed of 5 α-helices and 5 β-sheets; the DNA-binding domain contains an HTH (helix-turn-helix) motif, including 4 α-helices. Conversely, the C-terminal 3D (three-dimension) structure has not yet been resolved (28). In *B. abortus*, NtrX recognizes and binds via its HTH motif to a palindromic DNA sequence ($CAAN_{3\text{-}5}TTG$) in the *ntrY* promoter to directly regulate expression of *ntrY*(27, 28). In *S. meliloti*1021 strain, NtrX regulates cell growth, flagellum formation, motility, succinoglycan biosynthesis, nodulation and nitrogen fixation (29, 30). In the present study, we investigated the regulatory mechanism by which NtrX controls cell division of *S. meliloti*.

Results

Cell division defects of *S. meliloti ntrX* mutants.

We previously reported that NtrX regulates succinoglycan production, flagellum formation and cell motility in *S. meliloti* based on the data from the plasmid insertion mutant, SmLL1 (*ntrX18*)(29). After we carefully examined the cells from the continuous subculture of LB/MC, a few abnormal cells appeared under a light microscope and a transmission electron microscope (Fig. 1A-B), suggesting that NtrX contributes to bacterial cell division. To test this possibility, the synchronized cells from MOPS minimal broth were sub-cultured into LB/MC, and the collected cells were used for evaluation of genomic DNA content with flow cytometry. The results showed that genomic DNA content (the peak) of *S. meliloti* 1021 at the time of zero was similar to that of 3-hour cultures, and the peak of the 1.5th hour was between them (Fig. 1C). Interestingly, the peak of the *ntrX*18 cells at time of zero was close to that of *S. meliloti*1021, while the peaks after one and half hour and 3 hours culture were different from the wild type (Fig. 1C). Meanwhile, the peaks of the mutant cells are not similar at time zero compared with that of 3 hours culture. These results indicated that genomic DNA synthesis is affected by NtrX downregulation in the *ntrX*18 mutant.

To exclude the polar effect of *ntrX*18, we had to construct a depletion strain, since the *ntrX* deletion mutant has not successfully been screened(29). In this strain, the genomic *ntrX* gene has been deleted, and the vector of pSRK-Gm has shown to contain an *ntrX* gene in control of the promoter of *lacIQ*(31). Thus, the NtrX protein is expressed from the plasmid after induction of IPTG (isopropyl β-D-thiogalactoside). We observed that the depletion strain did not grow in LB/MC broth without IPTG, but it grew well after induction of 1 mM IPTG (Fig. 1D), indicating that NtrX is required for *S. meliloti* cell duplication. The depletion cells had elongated, branched or irregular shapes in the LB/MC subculture without IPTG, whereas after induction of IPTG in the broth, the cells took on a shape similar to those of *S. meliloti* 1021

(Fig.1E). The genomic DNA content of the depleted cells was evaluated by flow cytometry. It showed that over three peaks were found in cells without IPTG induction, but one main peak appeared from the cells induced by IPTG, especially after 2-hour IPTG treatment (Fig. 1F), suggesting that NtrX is essential for bacterial genomic DNA replication. These observations confirm that NtrX is a new regulator of bacterial cell division.

Expression of the CtrA system genes is regulated by NtrX in *S. meliloti* cells.

The defects of the *ntrX* mutants provided a possibility that NtrX regulates the cell cycle genes at transcriptional level. Quantitative RT-PCR (qRT-PCR) was employed to evaluate differential expression of cell cycle regulatory genes in LB/MC subcultures of synchronized *S. meliloti* cells. Transcript levels of *ntrX*, *pleC*, *gcrA* and *ccrM* have varied similarly in the wild-type cells, from increase to decrease during three hours (Fig. 2A). In contrast, transcript levels of *ctrA*, *dnaA*, *chpT*, *cpdR1 and ftsZ1* decreased at first, and then increased in the wild-type cells (Fig. 2A). Transcript levels of *ntrY*, a histine kinase gene appeared stable during three hours (Fig. 2A). These data suggested that expression of these genes (except *ntrY*) is in a cyclical manner. Transcripts of *ntrX*, *pleC*, *chpT*, *cpdR1*, *dnaA* and *ftsZ1* were significantly reduced in the *ntrX*18 cells compared with the wild-type (Fig. 2A), suggesting that NtrX is a positive transcription regulator for these genes. On the contrary, transcripts of *ntrY*, *gcrA*, *ccrM*, even and *ctrA* (except the first period) were significantly elevated in the mutant cells compared with the wild-type (Fig. 2A), suggesting that NtrX is a negative transcription regulator for these genes. Therefore, NtrX seems to control the cell cycle regulatory genes at transcriptional level in the reverse way.

To confirm the above results, transcript levels of above genes were evaluated in the *ntrX* depletion strain with or without IPTG induction by qRT-PCR. Transcripts of *ntrX* were enormously accumulated in the cells induced by IPTG (Fig. 2B). Correspondingly, transcripts of *pleC*, *chpT*, *cpdR1*, *dnaA* and *ftsZ1* significantly increased in the cells after 2 or 3-hour IPTG treatment compared with those cells without treatment (Fig. 2B). Meanwhile, transcription of *ntrY*, *ctrA*, *gcrA* and *ccrM* was significantly repressed after 2-hour IPTG treatment (Fig. 2B). Thus, the data from

the depletion strain is consistent with those from *ntrX18*.

The protein level of NtrX showed cyclical alterations in both cells of *S. meliloti* 1021 and *ntrX*18 from immune-blotting assays (Fig. 2C), supporting that NtrX is a transcriptional factor with a cyclical expression. NtrX proteins from the *ntrX*18 cells were less than those from *S. meliloti* 1021 (Fig. 2C), confirming that *ntrX*18 is a knock-down mutant. The CtrA protein level exhibited a similarly varied trend as reported in Sm1021 cells during 3 hours(32), whereas it apparently increased in those *ntrX*18 cells (Fig. 2C). Two forms of GcrA proteins were detected in *S. meliloti* cells using our anti-GcrA antibodies, and the smaller one could be digested proteins (Fig. 2C). The variation trends of GcrA larger protein from both Sm1021 and *ntrX*18 were similar to those of CtrA (Fig. 2C), confirming that NtrX represses the expression of *ctrA* and *gcrA* in *S. meliloti*. In the depletion cells, the levels of NtrX proteins apparently increased after IPTG induction (Fig. 2D). However, the protein levels of CtrA and GcrA apparently decreased in different extent (Fig. 2D). These data supported the conclusion that NtrX is a negative regulator for transcription of *ctrA* and *gcrA*.

To reconfirm that the expression of the CtrA system genes is regulated by NtrX, the promoter-*uidA* fusions were co-transformed with p*ntrX* or the empty vector（pSRK-Gm） into *E. coli* DH5α, respectively. X-Gluc staining showed that the activity of the promoter of *ctrA* or *gcrA* in the cells carrying p*ntrX* was weaker than those cells carrying pSRK-Gm (Fig. 3A). In contrast, the activity of the *dnaA* promoter is apparently elevated in the cells co-expressing *ntrX* compared with the control (Fig. 3A). These observations are consistent with quantitative analysis of GUS activities (Fig. 3B). These heterogeneous expression data supported the conclusion that NtrX negatively controls transcription of *ctrA* and *gcrA*, but positively regulates transcription of *dnaA*.

Multiple defects of *S. meliloti* 1021 expressing NtrX^{D53E}.

As a two-component response regulator, NtrX contains an N-terminal receiver domain and a C-terminal DNA-binding domain(28). An invariant aspartate residue (D53) in

the receiver domain is the phosphorylation site of the protein from *Brucella* and *Caulobacter* species(26, 28). To determine the function of the 53rd aspartate of NtrX from *S. meliloti*, we first attempted to construct its substitutions of alanine, asparagine or glutamate in *S. meliloti* 1021 genome, but no mutants were successfully obtained, just like construction of the *ntrX* deletion(29). Therefore, we had to construct recombinant plasmids for inducible expression of NtrX^{D53A}, NtrX^{D53N} or NtrX^{D53E}, and then introduced them respectively into *S. meliloti* by mating. Interestingly, many colonies containing p*ntrX*^{D53E} grew on LB/MC agar plates containing 0.1 M IPTG, whereas only a few colonies containing p*ntrX*^{D53A} or p*ntrX*^{D53N} were harvested (Fig. 6E), suggesting that the 53rd aspartate of NtrX is vital for cell duplication of *S. meliloti*. The strain of *S. meliloti* 1021/p*ntrX*^{D53E} was used for phenotype analyses subsequently. It grew slowly in LB/MC broth compared with the strain of *S. meliloti*1021/pSRK-Gm or *S. meliloti* 1021/p*ntrX* (Fig. 4A), confirming that NtrX^{D53E} disrupts cell division of *S. meliloti*. Meanwhile, the strain of *S. meliloti* 1021/p*ntrX*^{D53E} exhibited motility deficiency and overproduced succinoglycan (Fig. 4B), just like the mutant of *ntrX*18(29). Many abnormal cells (larger, longer and irregular) of the strain were clearly observed under a fluorescence microscope compared with the cells of *S. meliloti* 1021/pSRK-Gm (somewhat similar to the *ntrX*18 cells, Fig. S2A), after introducing a constitutive-expression GFP while *S. meliloti* 1021 cells expressing NtrX displayed normal shapes, and a few cells moved rapidly (Table S1). Flow cytometry data showed that the fluorescence curve of *S. meliloti*1021/pSRK-Gm or *S. meliloti*1021/p*ntrX* almost overlapped at time zero and at the 3rd hour, and it moved out at the 90th minute (Fig.4D). However, the fluorescence curves of *S. meliloti* 1021/p*ntrX*^{D53E} did not overlap, similar to those of *ntrX*18 with pSRK-Gm (Fig. 4D and Fig. S1B). These observations confirmed that the 53rd aspartate of NtrX is essential for cell division of *S. meliloti*.

Expression of cell cycle associated genes is disrupted by NtrX^{D53E} in *S. meliloti*.

The defects of cell division of *S. meliloti* 1021/p*ntrX*^{D53E} promoted us to evaluate the expression level of cell cycle related genes. The qRT-PCR assays showed that 0.1 M IPTG significantly induced transcription of *ntrX* or *ntrX*^{D53E} (Fig. 5A).

Correspondingly, the transcript levels of *ctrA*, *gcrA*, *minC* and *ntrY* decreased or showed a decreasing trend in the strain of *S. meliloti* 1021/p*ntrX* after treatment of IPTG compared with the cells without treatment, while those of *dnaA* and *ftsZ1* increased in the same condition (Fig. 5A), supporting the conclusion that NtrX negatively regulates transcription of *ctrA* and *gcrA*, but positively controls transcription of *dnaA*. In contrast, the transcript levels of *ctrA*, *gcrA*, *minC* and *ntrY* significantly increased in the strain of *S. meliloti* 1021/p*ntrX*^{D53E} after treatment of 0.1M IPTG, while those of *dnaA* and *ftsZ1* decreased in the same condition (Fig.5A), suggesting that NtrX^{D53E} disrupts regulation of the native NtrX protein in *S. meliloti*1021. Western blotting assays showed that more NtrX or NtrX^{D53E} proteins were induced after two-hour treatment of 0.1M IPTG, but the proteins of CtrA and GcrA apparently decreased in the strain of *S. meliloti* 1021/p*ntrX* (Fig. 5B). Interestingly, the protein level of CtrA and GcrA apparently increased in the strain of *S. meliloti* 1021/p*ntrX*^{D53E} after treatment of IPTG (Fig. 5B). These data are consistent with transcriptional results from qRT-PCR.

Phosphorylated NtrX regulates cell division of *Rhizobium* species.

The 3D structure of NtrX from *B. abortus* has been resolved by X-ray crystal diffraction(27, 28). It was successfully used for reconstruction of 3D structures of NtrX from *S. meliloti*, *Agrobacterium tumefacience* and *C. crescentus* in Swiss-Model server. The conserved NtrX receiver domains of the four bacterial species consist of five α-helixes and five β-sheets, linked with loops (Fig. 5A-B). The invariant 53rd aspartate residue is located at the end of the third β-sheet, which is attracted by the 105th lysine residue to form a salt bridge, together with the 9th and 10th aspartate residues, and the 11th glutamate residue for binding to one magnesium ion (Fig. 5B).

The purified NtrX and the NtrY kinase domain His-fusion proteins were used for phosphorylation assays in Phos-Tag gel *in vitro*, showing that NtrX was phosphorylated by NtrY (Fig. 6C). The phosphorylated NtrX proteins were clearly observed in *S. meliloti* 1021 cells in Phos-Tag gel and by immuno-blotting, but almost no phosphorylated proteins in *ntrX*18 cells were found because of less NtrX proteins (Fig. 6D). Levels of phosphorylated protein had apparently increased in *S. meliloti*

1021/p*ntrX* cells after 1-hour IPTG induction compared with those from *S. meliloti* 1021/p*ntrX*^{D53E} cells (Fig. 6D). The results indicated that the 53rd aspartate residue is the phosphorylation site of NtrX *in vivo*.

The mating tests showed that a lot of colonies expressing NtrX^{D53E} were formed on the plates containing 0.1 M IPTG; a few small colonies expressing NtrX^{D53A} were observed; almost no colonies were found on the same plates for the strain of *S. meliloti* 1021/p*ntrX*^{D53N} (Fig. 6E), indicating that the 53rd amino acid residue with negative charges is important for cell division. In contrast, expression of NtrX or NtrX^{D53E} repressed growth of *A. tumefaciens* C58, whereas expression of NtrX^{D53A} or NtrX^{D53N} did not (Fig. 6F). Meanwhile, expression NtrX^{D53A} or NtrX^{D53N} did not suppress succinoglycan production, but expression of NtrX or NtrX^{D53E} did in the strain (Fig. S3). Additionally, colonies of *C. crescentus* NA1000 carrying p*ntrX* were not successfully obtained on YEB agar plates, but many colonies containing p*ntrX*^{D53A}, p*ntrX*^{D53N} or p*ntrX*^{D53E} appeared on the plates (data not shown). These results suggest that the phosphorylated NtrX proteins play a distinct role in cell cycle regulation of *A. tumefaciens* and *C. crescentus* and *S. meliloti*.

NtrX recognizes a conserved promoter motif of cell cycle regulatory genes.

To systemically identify downstream genes directly regulated by NtrX, chromatin immunoprecipitation-DNA sequencing (ChIP-Seq) was performed using anti-NtrX antibodies. Total 82 DNA fragments were precipitated, with 12 and 10 DNA fragments from the symbiotic plasmids SymA and SymB, respectively, and 60 DNA fragments from Chromosome (Fig.7A and Table S2). We examined sequencing data for these fragments and found that the enriched DNA fragments included genes associated with cell cycle regulation, such as *ctrA*, *dnaA*, *ftsZ1*, *divL* and *cpdR1*, some of which are presented as peak maps in Fig. 7B. These results suggest that the promoters of several cell cycle-related genes are specifically recognized *in vivo* by NtrX. To verify the ChIP-Seq results, each DNA fragment precipitated by anti-NtrX antibodies was evaluated by quantitative PCR, and the results were largely consistent. For example, the promoter fragments of *ctrA*, *dnaA*, *cpdR1*, *divL*, *ftsZ1* and *ntrY* were significantly enriched by anti-NtrX antibodies (Fig. 7C), whereas that of *minC* was

not. These results indicate that NtrX directly interacts with promoter DNA of several cell cycle regulatory genes.

To identify the conserved motif recognized by NtrX, the ChIP-Seq data were analyzed using the MEME program, revealing the presence of the motif CAANxTTG in some of the precipitated DNA regions. This motif matches the *cis*-elements ($CAAN_{3\text{-}5}TTG$) in the *ntrY* promoter recognized by NtrX from *B. abortus*, as based on foot-printing results (28). The motif was then used as a query to scan all gene promoter regions in the entire genome of *S. meliloti* 1021 using the genome-scan dna-pattern program on the RSAT server (http://embnet.ccg.unam.mx/rsat). According to the results, there are 2155 $CAAN_{(1\text{-}5)}TTG$ motifs, of which 51.5% (1111) are located on Chromosome and 25.0% (539) and 23.5% (508) are located on the symbiotic plasmids SymA and SymB respectively, including 358 $CAAN_3TTG$, 529 $CAAN_4TTG$, and 548 $CAAN_5TTG$ motifs (Fig. 8A). Moreover, 14 motifs were found in the promoter regions of cell cycle regulatory genes, such as the cell cycle-regulating transcription factor genes *ctrA*, *gcrA*, and *dnaA*, response regulator genes *chpT* and *cpdR1*, histidine kinase genes *divL*, *cckA*, *cbrA*, and *pleC*, and the Z-ring formation gene *ftsZ1* (Fig. 8B and Table S3).

To confirm whether the $CAAN_{3\text{-}5}TTG$ motifs in the *ntrY* gene promoter of *S. meliloti* are recognized by the NtrX protein, as in *B. abortus*(28), we synthesized biotinylated 80-bp DNA probes (containing two conserved motifs of **CAA**CACCG**TTG** and **CAA**TGCG**TTG**) for gel retardation assays (Table S4). The results indicated the formation of two protein-DNA complexes (Fig. 8C), which suggests that the binding between NtrX and *ntrY* promoter is conserved in bacteria. To determine the importance of NtrX phosphorylation for target DNA binding, we replaced NtrX with $NtrX^{D53E}$ and then performed gel retardation assays. As almost no protein-DNA complex has been formed (Fig. 8C), it seems that only phosphorylated NtrX can efficiently bind to the *ntrY* promoter. We used the same approach to analyze the interaction between the NtrX protein and the *dnaA* promoter (a 75-bp DNA fragment containing the motif **CAA**AACCC**TTG**) *in vitro* and found specific complex formation with phosphorylated NtrX (Fig. 8E). To determine the functional

importance of conserved nucleotides in CAAN$_{1-5}$TTG, we replaced A/T bases in the **CAA**AACCC**TTG** sequence of the *dnaA* promoter probe with G/C (**CGG**AACCC**CCG)** and then performed gel retardation assays. The results showed a little DNA-protein complex formation between phosphorylated NtrX and the probe harboring the replaced bases (Fig. 8E), indicating that the conserved A/T bases in the motif are essential for the NtrX-DNA interaction. We also examined the interaction between the *S. meliloti ctrA* gene promoter and the NtrX protein via the same approach and found that phosphorylated NtrX formed a specific complex with the DNA probe (containing the **CAA**CC**TTG** motif) (Fig.8D). In addition, phosphorylated NtrX protein bound specifically to the promoter fragments of the *gcrA* and *ftsZ1* genes (containing motifs **CAA**ACC**TTG** and**CAA**C**TTG**, respectively) (Fig. 8F and S2). These results reveal that phosphorylated NtrX proteins can directly bind to promoter regions containing CAAN$_{1-5}$TTG motifs from several cell cycle regulatory genes.

Distribution of NtrX binding sites in other α-proteobacteria.

NtrX may work as a cell cycle transcriptional regulator in other α-proteobacteria, such as *A. tumefaciens*, *B. abortus* and *C. crescentus.* This possibility is supported by the NtrX binding site analyses. Using the genome-scan dna-pattern program on the RSAT server (http://embnet.ccg.unam.mx/rsat), the motifs of NtrX in the whole-genome wide of other three α-proteobacterial species showed that there are 1384, 2037 and 2562 CAAN $_{(1-5)}$TTG motifs in *C. crescntus*, *B. abortus* and *A. tumefaciens*, respectively. The promoters of conserved cell cycle regulatory genes were carefully scanned, showing that the promoter regions of *divJ*, *gcrA* and *ccrM* contain 1-2 motifs of CAAN$_{(1-5)}$TTG in *C. crescentus*, four NtrX binding motifs in the promoter regions of *divK*, *gcrA*, *dnaA* and *rcdA* in *B. abortus*, and nine motifs in the promoter regions of *ctrA, dnaA, gcrA, ftsZ1* and *ftsZ2* in *A. tumefaciens* respectively (Fig. S4). These data provide a new cue to study the conservatism of cell cycle regulation mediated by NtrX in α-proteobacteria.

Discussion

In several bacteria, NtrX is believed to be a response regulator of nitrogen metabolism(17-20, 23, 25), though it is associated with stability of CtrA (a determinant of cell cycle regulation in α-proteobacteria) in *E. chaffeensis*(25). Many bacterial mutants associated with *ntrX* have been found to grow slowly, but the hiding control mechanism remained largely unknown. In the present study, we find that NtrX works as a key transcriptional factor to control expression of the CtrA system genes (such as *ctrA*, *gcrA*, *dnaA*, *cpdR1* and *divL*) and *ftsZ1* by recognizing a conserved motif (CAANxTTG) in the target promoters (Fig. 9). Our findings reveal that NtrX regulates bacterial cell division at the transcriptional level in the manner of multiple targets. Therefore, NtrX may be the regulatory linker of nitrogen metabolism and cell division.

According to literatures and our genetic and biochemical data, NtrX is not only the regulator of nitrogen metabolism, but also involved in metabolic regulation of carbon sources, oxygen gas, energy and even many macromolecules (protein, DNA, RNA and succinoglycan) (21, 23-25, 29, 33). The diverse functions of NtrX in bacteria could result from the transcriptional control of numerous genes. Many of them could be directly regulated by NtrX, since their promoters contain one conserved recognition site (CAANxTTG) at least (Table S3). Transcriptional regulation of these genes mediated by NtrX is needed to be further investigated.

NtrX is a novel cell cycle regulator in bacteria. This conclusion is supported by genetic and biochemical evidence. First, three groups of genetic materials were used for analyses of cell division defects and cell cycle regulatory gene expression, such as the plasmid insertion mutant *ntrX*18(29), the *ntrX* depletion strain (Δ*ntrX*/pP*lac-ntrX*) and *S. meliloti* 1021/p*ntrX*^{D53E}. All three strains showed the consistent phenotypes of cell division, including slow growth, irregular cell shape, and genomic DNA increase (Fig. 1, 4 and 6). The defects of these strains may result from differential gene expression of cell cycle genes compared with their parent strains (Fig. 2, 3 and 5). From the expression data, we conclude that NtrX positively regulates transcription of

dnaA, but negatively controls expression of *ctrA* and *gcrA*. Therefore, NtrX may be an S-phase promoting regulator, since more S-phase cells were observed with overexpression of *ntrX* in *S. meliloti* 1021(Fig. 4D). Although the transcriptional control of these cell cycle genes is mediated by NtrX-promoter direct interactions (Fig. 7-8), the details that key amino acid residues of the protein interact the vital bases (CAA or TTG) of the promoter will be further investigated.

Cell cycle regulation of NtrX may be not restricted in *S. meliloti*. This deduction is supported by the reverse genetic data from *A. tumefaciens*, though the regulation could be different (Fig. 6F and S4-5). An *ntrX* deletion mutant of *C. crescentus* was reported to not affect bacterial growth in the exponential phase(26). It is possible that the NtrX homologue does not function in the condition, as it affected cell growth by acid treatment(26). Noticeably, the amino acid sequence of NtrX from *C. crescentus* is very different from those of *B. abortus*, *A. tumefaciens* and *S. meliloti* (Fig. 6A), which could influence the protein function. Additionally, differential expression of cell cycle regulatory genes and distinct NtrX binding sites in their promoters (Fig.S4) could be associated with the function of NtrX homologues. Thus, NtrX-mediated cell cycle regulation may be plastic in α-proteobacteria.

The 53rd aspartate residue is the phosphorylation site of NtrX (Fig. 6C-D), which is required for cell division in *S. meliloti* (Fig.4-5 and 6E). From the 3D structure reconstructed, this residue may form a salt bridge with the 105th lysine (Fig. 6B). After it is phosphorylated, the salt bridge could be strengthened to change the conformation of the protein. Biochemical evidence *in vitro* confirmed that NtrY phosphorylates NtrX (Fig. 6C), but the histidine kinase that phosphorylates it *in vivo* is not identified. It is possible that NtrX is phosphorylated by several histidine kinases that are able to perceive environmental cues, since over two histidine kinases can phosphorylate *in vitro* a response regulator from *C. crescentus*(2). Our previous data also showed that NtrY is not associated with NtrX-mediated regulation of motility, succinoglycan production or symbiotic nitrogen fixation(29), meaning NtrX may interact with other histidine kinases. We know that NtrX serves as a response regulator of nitrogen metabolism in several bacterial species, whereas NtrY appears to

be a sensor of oxygen in *B. abortus*(23). Therefore, nitrogen nutrient signals may be perceived by the conserved NtrB/NtrC system, and then delivered to NtrX for reprogramming downstream gene expression.

As *S. meliloti* is a symbiont of *Medicago* plants such as alfalfa, NtrX-mediated cell cycle regulation may occur in infected plant cells because the bacterial cells duplicate in infection threads and in infected nodule plant cells, and the *ntrX*18 mutant showed a sever deficiency of symbiosis(29).

Materials and Methods

Strains and culture medium

Escherichia coli DH5α and BL21 were cultured in LB medium at 37°C. *S. meliloti* strains (Sm1021, *ntrX*18 or SmLL1 and derivatives) (29) were cultured in LB/MC medium at 28°C. MOPS-GS broth was utilized for cell synchronization of *S. meliloti* strains (34). *A. tumefaciens* C58 was cultured in LB medium at 28 °C, whereas *C. crescentus* N1000 was cultured in YEB medium at 28 °C. The following antibiotics were added to media: kanamycin, 50 μg/ml; gentamicin, 10 μg/ml; chloramphenicol, 30 μg/ml; neomycin, 200 μg/ml; streptomycin, 200 μg/ml; tetracycline, 10 μg/ml.

Recombinant plasmid construction

Primers P*ntrX*1 and P*ntrX*2 carrying *Hind*III and *Xba*I digestion sites were used to amplify the *S. meliloti ntrX* gene (Table S4). The overlapping PCR primers NMF and NMR were used to amplify the *ntrX* gene fragment with substitution of aspartate with glutamate, asparagine or alanine (Table S4). Overlapping PCR was performed as described by Wang, 2013 (29). The PCR products were digested with *Hind*III and *Xba*I (Thermo) and ligated with digested pSRK-Gm(31) to obtain the recombinant plasmids p*ntrX*, p*ntrX*^{D53E}, p*ntrX*^{D53A} and p*ntrX*^{D53N}. The depletion strain was screened on LB/MC agar plates containing 1mM IPTG after introduction of p*ntrX* into *ntrX*18. Primers of P*ntrY*k1, P*ntrY*k2, P*ntrX*1^{D53E}, P*ntrX*2^{D53E}, P*ctrA*1, P*ctrA*2, P*gcrA*1 and P*gcrA*2 were used for amplification of the NtrY kinase encoding region,

450 *ntrX*^{D53E}, *ctrA* and *gcrA*, respectively (Table S4). The PCR fragments were digested
451 by appropriate restriction enzymes and ligated into pET28b to harvest p*ntrY*k,
452 p*ntrX*^{D53E}, p*ctrA* and p*gcrA* for recombinant protein purification. Primers of P*ctrA*p1,
453 P*ctrA*p2, P*gcrA*p1, P*gcrA*p2, P*dnaA*p1 and P*dnaA*p2 were used for amplification the
454 promoter regions of the *ctrA*, *gcrA* and *dnaA*, respectively (Table S4). The PCR
455 fragments were digested by appropriate restriction enzymes and ligated into pRK960
456 to gain the recombinant plasmids p*PctrA*, p*PgcrA* and p*PdnaA*.

457 **Bacterial cell synchronization**

458 The method of De Nisco was used for bacterial cell synchronization (34). A sample of
459 *S. meliloti* cells were selected from an agar plate, placed in 5 ml LB/MC broth and
460 grown overnight. A 100-μl aliquot of bacterial culture was transferred to 100 ml
461 LB/MC broth and incubated overnight until OD_{600}=0.1-0.15; the culture was
462 centrifuged (6, 500 rpm, 5 min, 4 °C), and the cell pellet was washed twice with
463 sterilized 0.85% NaCl solution. The cells were resuspended in MOPS-GS
464 synchronization medium and grown at 28°C for 270 min. After centrifugation, the
465 cells were washed twice with sterilized 0.85% NaCl solution, resuspended in LB/MC
466 broth, and cultured at 28°C. Synchronically cultivated bacterial cells were collected
467 every 30 min (within 3 hours).

468 **RNA extraction and purification**

469 Twenty milliliters of bacterial culture (OD_{600}≈0.8) was collected by centrifugation (6,
470 000 rpm, 5 min, 4°C), and the cells were washed twice with DEPC-treated water.
471 RNA extraction was performed using 1 ml of Trizol (Life Technology) for RNA
472 extraction, and its purification was performed as described by Wang, 2013 (29).

473 **qRT-PCR and qPCR**

474 RNA reverse transcription was performed using PrimeScript RT reagent Kit with
475 gDNA Eraser (TaKaRa). The qPCR reaction system included the following: SYBR®
476 Green Real-time PCR Master Mix, 4.75 μl; cDNA or DNA, 0.25 μl; 10 pmol/μl
477 primers, 0.5 μl; ddH2O, 4.5 μl. The reaction procedure was as follows: 95°C, 5 min;
478 95°C, 30 s; 55°C, 30 s; 72°C, 1 kb/min. The selected reference gene was Smc00128.
479 The $2^{-\Delta\Delta}$CT method was applied for analysis of gene expression levels. All primers

are listed in Table S4.

Chromatin immunoprecipitation (ChIP)

ChIP was performed as described by Pini (32). Anti-NtrX antibodies prepared by Wenyuange (Shanghai) were used for ChIP assays(35).

Flow cytometry

Four milliliters of fresh bacterial culture (OD_{600} = 0.3) was centrifuged (6, 000 rpm, 5 min, 4°C), and the cell pellets were washed twice with 0.85% NaCl solution (stored at 4°C). The flow cytometry protocol of De Nisco was used (34). Each sample was assessed using a MoFlo XDF (Beckman Coulter) flow cytometer, and the results were analyzed using Summit 5.1 software (Beckman Coulter).

EMSA (electrophoretic mobility shift assay)

EMSA was performed as described by Zeng (35). LightShift™ Chemiluminescent EMSA Kit (ThermoFisher) was applied in the assays. Probes for *ntrY*, *ctrA*, *dnaA*, *gcrA*, *ftsZ1* and *visN* promoter DNA labeled with biotin were synthesized (Invitrogen); the probes are listed in Table S4. Phosphorylated NtrXr proteins (from Ni^{2+} column purification) used in these assays were prepared. 6 μg of purified protein was mixed with 2 mM of acetyl phosphate (Sigma) in 100 μl of phosphorylation buffer (50 mM Tris-HCl pH7.6, 50mM KCl, 20 mM $MgCl_2$), and incubated at 28 °C for one hour. Acetyl phosphate was removed using an ultra-filtration tube (Millipore), resolved in 100 μl of phosphorylation buffer.

β-glucuronidase activity assay

Activity assays of p*PctrA-uidA*, p*PgcrA-uidA* and p*PdnaA-uiA* in *E. coli* DH5 were performed as described by Tang (36).

NtrX phosphorylation assay

1 mg of His-NtrX fusion protein (NtrXr), and 1 mg of His-NtrY kinase domain fusion protein (NtrY-Kr) purified through Ni^{2+} column were used for NtrX phosphorylation assays *in vitro*. 2 mM of acetyl phosphate (Sigma) was mixed with 300 μg of NtrY-Kr in 1 ml of phosphorylation buffer, and then incubated at room temperature for one hour. Acetyl phosphate was removed using an ultra-filtration tube (Millipore), resolved in 1 ml of phosphorylation buffer. 1, 3 and 10 μg of phosphorylated NtrY-Kr

protein was added into 200 μl of phosphorylation buffer with 10 μg of NtrXr, and incubated at 28 °C overnight. The samples were separated by Phos-Tag gel (Mu Biotechnology, Guangzhou). Phosphorylated NtrX levels from *S. meliloti* cells were separated in Phos-Tag gel. *S. meliloti* 1021 carrying p*ntrX* or p*ntrX*^{D53E} was cultured in LB/MC broth induced by 1mM IPTG for 1 to 3 hours. ~1 μg total protein was input for each sample. All proteins were transferred onto PVDF, and then detected by anti-NtrX antibodies from Western blotting assays (13).

Western blotting

Western blotting was performed as described by Tang (37). Proteins were detected using an ECL fluorescence colorimetric kit (Tiangen) and visualized using a Bio-Rad Gel Doc XR. Anti-NtrX antibodies were prepared in Wenyuange, Shanghai, China(35); anti-eGFP antibodies were purchased from Thermo. Anti-CtrA and anti-GcrA antibodies were prepared by Hua'an Biotech, Hangzhou, China.

Microscopy

A 5-μl aliquot of fresh *S. meliloti* culture (OD_{600} = 0.15) was placed on a glass slide and covered with a cover glass. The slide was slightly baked for a few seconds near the edge of the flame of an alcohol lamp. Cells expressing the pHC60 plasmid were observed in GFP mode (38), and images were acquired using a CCD camera Axiocam 506 color (Zeiss). The exposure time was set to 10 ms and 1,000 ms in order to capture bacterial morphology and motility, respectively. The images were analyzed with ZEN 2012 software (Zeiss).

The scanning electron microscopy, assays of cell motility in LB/MC swarming plates and succiniglycan production on calcoflour plates were performed as Wang (29).

ChIP sequencing and bioinformatic analysis

ChIP-Seq were performed by Bohao Biotech, Shanghai. The original genome data of *S. meliloti* 1021 were obtained from NCBI. The sequencing data were analyzed by Bohao Biotech, Shanghai. . IGV software was employed to assess specific enrichment data based on ChIP-Seq results, and screenshots were generated for peak maps (39).Genome-wide $CAAN_{1\text{-}6}TTG$ *cis*-acting elements of bacteria were evaluated using the genome-scan dna pattern program on the RAST online server

(http://embnet.ccg.unam.mx/rsat) (40). The BDGP program was applied for promoter prediction (http://www.fruitfly.org/seq_tools/promoter.html)

Protein 3D structure analysis

The NtrX protein 3D structure was reconstructed in Swiss-Model using the template of 4d6y (the 3D structure of the NtrX receiver domain from *Brucella*) in PDB (41). The 3D structure of the NtrX receiver domains were analyzed by Pymol (Delano Scientific).

Acknowledgments

This research was supported by the Natural Science Foundation of China (31570241 to L.L). We thanks to Dr. Urs Jena for providing the strain of *C. crescentus* N1000, and Dr. Yiwen Wang (Eastern Normal University) for help of SEM.

References

1. Laub MT, McAdams HH, Feldblyum T, Fraser CM, Shapiro L. 2000. Global analysis of the genetic network controlling a bacterial cell cycle. Science 290:2144-8.
2. Skerker JM, Laub MT. 2004. Cell-cycle progression and the generation of asymmetry in Caulobacter crescentus. Nat Rev Microbiol 2:325-37.
3. Laub MT, Shapiro L, McAdams HH. 2007. Systems biology of Caulobacter. Annu Rev Genet 41:429-41.
4. Panis G, Murray SR, Viollier PH. 2015. Versatility of global transcriptional regulators in alpha-Proteobacteria: from essential cell cycle control to ancillary functions. FEMS Microbiol Rev 39:120-33.
5. Jacobs C, Ausmees N, Cordwell SJ, Shapiro L, Laub MT. 2003. Functions of the CckA histidine kinase in Caulobacter cell cycle control. Molecular Microbiology 47:1279-1290.
6. Biondi EG, Reisinger SJ, Skerker JM, Arif M, Perchuk BS, Ryan KR, Laub MT. 2006. Regulation of the bacterial cell cycle by an integrated genetic circuit. Nature 444:899-904.
7. Jones KM, Kobayashi H, Davies BW, Taga ME, Walker GC. 2007. How rhizobial symbionts invade plants: the Sinorhizobium-Medicago model. Nature Reviews Microbiology 5:619-633.
8. Van de Velde W, Zehirov G, Szatmari A, Debreczeny M, Ishihara H, Kevei Z, Farkas A,

Mikulass K, Nagy A, Tiricz H, Satiat-Jeunemaitre B, Alunni B, Bourge M, Kucho K, Abe M, Kereszt A, Maroti G, Uchiumi T, Kondorosi E, Mergaert P. 2010. Plant peptides govern terminal differentiation of bacteria in symbiosis. Science 327:1122-6.

9. Farkas A, Maroti G, Durgo H, Gyorgypal Z, Lima RM, Medzihradszky KF, Kereszt A, Mergaert P, Kondorosi E. 2014. Medicago truncatula symbiotic peptide NCR247 contributes to bacteroid differentiation through multiple mechanisms. Proc Natl Acad Sci U S A 111:5183-8.
10. Penterman J, Abo RP, De Nisco NJ, Arnold MF, Longhi R, Zanda M, Walker GC. 2014. Host plant peptides elicit a transcriptional response to control the Sinorhizobium meliloti cell cycle during symbiosis. Proc Natl Acad Sci U S A 111:3561-6.
11. Montiel J, Downie JA, Farkas A, Bihari P, Herczeg R, Balint B, Mergaert P, Kereszt A, Kondorosi E. 2017. Morphotype of bacteroids in different legumes correlates with the number and type of symbiotic NCR peptides. Proc Natl Acad Sci U S A 114:5041-5046.
12. Kobayashi H, De Nisco NJ, Chien P, Simmons LA, Walker GC. 2009. Sinorhizobium meliloti CpdR1 is critical for co-ordinating cell cycle progression and the symbiotic chronic infection. Molecular Microbiology 73:586-600.
13. Pini F, Frage B, Ferri L, De Nisco NJ, Mohapatra SS, Taddei L, Fioravanti A, Dewitte F, Galardini M, Brilli M, Villeret V, Bazzicalupo M, Mengoni A, Walker GC, Becker A, Biondi EG. 2013. The DivJ, CbrA and PleC system controls DivK phosphorylation and symbiosis in Sinorhizobium meliloti. Molecular Microbiology 90:54-71.
14. Xue S, Biondi EG. 2018. Coordination of symbiosis and cell cycle functions in Sinorhizobium meliloti. Biochim Biophys Acta doi:10.1016/j.bbagrm.2018.05.003.
15. Robinson MD, Oshlack A. 2010. A scaling normalization method for differential expression analysis of RNA-seq data. Genome Biology 11.
16. Schallies KB, Sadowski C, Meng JL, Chien P, Gibson KE. 2015. Sinorhizobium meliloti CtrA Stability Is Regulated in a CbrA-Dependent Manner That Is Influenced by CpdR1. Journal of Bacteriology 197:2139-2149.
17. Pawlowski K, Klosse U, de Bruijn FJ. 1991. Characterization of a novel Azorhizobium caulinodans ORS571 two-component regulatory system, NtrY/NtrX, involved in nitrogen fixation and metabolism. Mol Gen Genet 231:124-38.
18. Nogales J, Campos R, BenAbdelkhalek H, Olivares J, Lluch C, Sanjuan J. 2002. Rhizobium tropici genes involved in free-living salt tolerance are required for the establishment of efficient nitrogen-fixing symbiosis with Phaseolus vulgaris. Mol Plant Microbe Interact 15:225-32.
19. Ishida ML, Assumpcao MC, Machado HB, Benelli EM, Souza EM, Pedrosa FO. 2002. Identification and characterization of the two-component NtrY/NtrX regulatory system in Azospirillum brasilense. Braz J Med Biol Res 35:651-61.
20. Bonato P, Alves LR, Osaki JH, Rigo LU, Pedrosa FO, Souza EM, Zhang N, Schumacher J, Buck M, Wassem R, Chubatsu LS. 2016. The NtrY-NtrX two-component system is involved in controlling nitrate assimilation in Herbaspirillum seropedicae strain SmR1. FEBS J 283:3919-3930.
21. Gregor J, Zeller T, Balzer A, Haberzettl K, Klug G. 2007. Bacterial regulatory networks include direct contact of response regulator proteins: Interaction of RegA and NtrX in Rhodobacter capsulatus. Journal of Molecular Microbiology and Biotechnology 13:126-

139.

22. Lemmer KC, Alberge F, Myers KS, Dohnalkova AC, Schaub RE, Lenz JD, Imam S, Dillard JP, Noguera DR, Donohue TJ. 2020. The NtrYX Two-Component System Regulates the Bacterial Cell Envelope. mBio 11.
23. Carrica MD, Fernandez I, Marti MA, Paris G, Goldbaum FA. 2012. The NtrY/X two-component system of Brucella spp. acts as a redox sensor and regulates the expression of nitrogen respiration enzymes. Molecular Microbiology 85:39-50.
24. Atack JM, Srikhanta YN, Djoko KY, Welch JP, Hasri NHM, Steichen CT, Hoven RNV, Grimmond SM, Othman DSMP, Kappler U, Apicella MA, Jennings MP, Edwards JL, McEwan AG. 2013. Characterization of an ntrX Mutant of Neisseria gonorrhoeae Reveals a Response Regulator That Controls Expression of Respiratory Enzymes in Oxidase-Positive Proteobacteria. Journal of Bacteriology 195:2632-2641.
25. Cheng Z, Lin M, Rikihisa Y. 2014. Ehrlichia chaffeensis proliferation begins with NtrY/NtrX and PutA/GlnA upregulation and CtrA degradation induced by proline and glutamine uptake. MBio 5:e02141.
26. Fernandez I, Sycz G, Goldbaum FA, Carrica MD. 2018. Acidic pH triggers the phosphorylation of the response regulator NtrX in alphaproteobacteria. Plos One 13.
27. Fernandez I, Otero LH, Klinke S, Carrica MD, Goldbaum FA. 2015. Snapshots of Conformational Changes Shed Light into the NtrX Receiver Domain Signal Transduction Mechanism. Journal of Molecular Biology 427:3258-3272.
28. Fernandez I, Cornaciu I, Carrica MD, Uchikawa E, Hoffmann G, Sieira R, Marquez JA, Goldbaum FA. 2017. Three-Dimensional Structure of Full-Length NtrX, an Unusual Member of the NtrC Family of Response Regulators. Journal of Molecular Biology 429:1192-1212.
29. Wang D, Xue H, Wang Y, Yin R, Xie F, Luo L. 2013. The Sinorhizobium meliloti ntrX gene is involved in succinoglycan production, motility, and symbiotic nodulation on alfalfa. Appl Environ Microbiol 79:7150-9.
30. Calatrava-Morales N, Nogales J, Ameztoy K, van Steenbergen B, Soto MJ. 2017. The NtrY/NtrX System of Sinorhizobium meliloti GR4 Regulates Motility, EPS I Production, and Nitrogen Metabolism but Is Dispensable for Symbiotic Nitrogen Fixation. Mol Plant Microbe Interact 30:566-577.
31. Khan SR, Gaines J, Roop RM, 2nd, Farrand SK. 2008. Broad-host-range expression vectors with tightly regulated promoters and their use to examine the influence of TraR and TraM expression on Ti plasmid quorum sensing. Appl Environ Microbiol 74:5053-62.
32. Pini F, De Nisco NJ, Ferri L, Penterman J, Fioravanti A, Brilli M, Mengoni A, Bazzicalupo M, Viollier PH, Walker GC, Biondi EG. 2015. Cell Cycle Control by the Master Regulator CtrA in Sinorhizobium meliloti. Plos Genetics 11.
33. Langmead B, Trapnell C, Pop M, Salzberg SL. 2009. Ultrafast and memory-efficient alignment of short DNA sequences to the human genome. Genome Biol 10:R25.
34. De Nisco NJ, Abo RP, Wu CM, Penterman J, Walker GC. 2014. Global analysis of cell cycle gene expression of the legume symbiont Sinorhizobium meliloti. Proc Natl Acad Sci U S A 111:3217-24.
35. Zeng S, Xing S, An F, Yang X, Yan J, Yu L, Luo L. 2020. Sinorhizobium meliloti NtrX interacts with different regions of the visN promoter. Acta Biochim Biophys Sin (Shanghai)

52:910-913.
36. Tang G, Wang Y, Luo L. 2014. Transcriptional regulator LsrB of Sinorhizobium meliloti positively regulates the expression of genes involved in lipopolysaccharide biosynthesis. Appl Environ Microbiol 80:5265-73.
37. Tang G, Xing S, Wang S, Yu L, Li X, Staehelin C, Yang M, Luo L. 2017. Regulation of cysteine residues in LsrB proteins from Sinorhizobium meliloti under free-living and symbiotic oxidative stress. Environ Microbiol 19:5130-5145.
38. Cheng HP, Walker GC. 1998. Succinoglycan is required for initiation and elongation of infection threads during nodulation of alfalfa by Rhizobium meliloti. Journal of Bacteriology 180:5183-5191.
39. Thorvaldsdottir H, Robinson JT, Mesirov JP. 2013. Integrative Genomics Viewer (IGV): high-performance genomics data visualization and exploration. Briefings in Bioinformatics 14:178-192.
40. van Helden J. 2003. Regulatory sequence analysis tools. Nucleic Acids Res 31:3593-6.
41. Arnold K, Bordoli L, Kopp J, Schwede T. 2006. The SWISS-MODEL workspace: a web-based environment for protein structure homology modelling. Bioinformatics 22:195-201.

Legends

Fig. 1. Cell division defects of the *S. meliloti ntrX* mutants in LB/MC medium.

(**A, E**) Cell shapes of the *ntrX* mutants under a light microscope or (**B**) a scanning electron microscope. Red arrows, abnormal cells; bars, 2μm. (**C, F**) Genomic DNA content of the *ntrX* mutants determined by flow cytometry. (**D**) Growth curve of the *ntrX* depletion strain in presence of 1 mM IPTG (the blue curve) and in absence of IPTG (the red curve). *ntrX*18, SmLL1(29), *ntrX*::pK18*mobsacB*; the *ntrX* depletion strain was used in D and F.

Fig. 2. Differential expression of the CtrA system genes in the *ntrX* mutants.

(**A-B**) Transcript levels of the CtrA system genes in the *ntrX* mutants evaluated by qRT-PCR. Error bars, ±SD. Student's t-test was used for significance evaluation. *, $P<0.05$. **, $P<0.001$. (**C-D**) Protein levels of NtrX, CtrA and GcrA in the *ntrX* mutant evaluated by Western blotting. The *ntrX* depletion strain was used in the experiment of B and D. All experiments were repeated twice.

Fig. 3. *S. meliloti* NtrX heterogeneously regulates expression of the CtrA system genes in *E. coli*.

(**A**) GUS staining results of *E. coli* DH5α colonies containing the promoter-*uidA* fusion on LB plates. (**B**) GUS activity level of *E. coli* DH5α cells containing the promoter-*uidA* fusion in LB broth. Error bars, ±SD. Student's t-test was used for significance evaluation. *, P<0.05. All experiments were repeated twice.

Fig. 4. Cell division defects of *S. meliloti* 1021 expressing NtrX^{D53E}.

(**A**) Growth curve of *S. meliloti* 1021 expressing NtrX^{D53E}. Error bars, ±SD. (**B**) Motility and succinoglycan production of *S. meliloti* 1021 expressing NtrX^{D53E}. (**C**) Cell shapes of *S. meliloti*1021 expressing NtrX^{D53E} under a fluorescence microscope. Bars, 100 μm. (**D**) Fluorescence intensity of *S. meliloti* 1021 expressing NtrX or NtrX^{D53E} determined by flow cytometry. Each strain carried the plasmid pHC60 for constitutive expression of GFP(38). All experiments were repeated twice.

Fig. 5. Differential expression of the CtrA system genes in *S. meliloti* 1021/ p*ntrX*^{D53E}.

(A) Transcript levels of the CtrA system genes in *S. meliloti*1021/ p*ntrX*^{D53E} evaluated by qRT-PCR. Error bars, ±SD. Student's t-test was used for significance evaluation. *, P<0.05. (B) Protein levels of NtrX, CtrA and GcrA in *S. meliloti* cells evaluated by Western blotting. -, without IPTG induction; +, treatment of 1 mM IPTG for 1, 2 and 3 hours. All experiments were repeated twice.

Fig. 6. Function of the 53rd aspartate residue in the NtrX receiver domain.

(**A**) Alignment of f NtrX receiver domain from four bacterial species. The amino acid sequence of each protein was obtained from NCBI. The secondary structures of the receiver domain were shown as green lines (loops), yellow arrows (β- sheets) and red bars (α-helixes). Ba2308, *Brucella abortus* biovar 1 str. 2308; Sm1021, *Sinorhizobium meliloti* 1021; AtC58, *Agrobacterium tumefaciens* C58; CcN1000, *Caulobacter*

crescentus N1000. (**B**) 3D structures of NtrX receiver domain from three bacterial species were reconstructed using *B. abortus* homolog protein (PDB:4d6y) as a template in Swiss-Model. Electrostatic interactions of the carboxyl group from the conserved 53rd aspartate residues were shown as Arabic number by Pymol. (**C**) NtrX phosphorylation catalyzed by the NtrY kinase domain *in vitro*. NtrY-Kr, His-NtrY kinase domain fusion protein ; NtrXr-P, phosphorylated NtrXr; Ac-Pi, acetyl phosphate. (**D**) Phosphorylated NtrX proteins from *S. meliloti* cells detected in Phos-Tag gel and by Western blotting. *S. meliloti* 1021 carrying p*ntrX* or p*ntrX*^{D53E} was cultured in LB/MC broth induced by 1mM IPTG for 1 to 3 hours. ~ 1 μg total protein was input for each sample. (**E**) Colonies of *S. meliloti* 1021 expressing the NtrX substitution of D53 on LB/MC plates. (**F**) Colonies of *A. tumefaciens* C58 expressing the NtrX substitution of D53 on LB plates.

Figure 7. NtrX directly interacts with the promoters of the cell cycle regulatory genes *in vivo*.

(**A**)Genome-wide distribution of DNA fragments specifically precipitated by anti-NtrX antibodies via ChIP-Seq. The cutoff value is 1600 reads. (**B**) Peak maps of the promoter regions for a few cell cycle regulatory genes from the DNA fragments specifically precipitated by anti-NtrX antibodies. Red bars indicate the putative recognition sites (CAAN$_x$TTG) of NtrX. (**C**) Abundance of DNA fragments specifically precipitated by anti-NtrX antibodies, as determined by qPCR. Error bars, ±SD. Student's t-test was used for significance evaluation. *, P<0.05. The experiment was repeated twice.

Fig. 8. NtrX interacts with the promoters of the cell cycle regulatory genes by recognizing a conserved *cis*-element.

(**A**) Statistics of NtrX recognition motifs (CAANxTTG) by scanning the genome of *S. meliloti*1021 in Regulatory Sequence Analysis Tool (RSAT). (**B**) The conserved motif CAAN $_{(1\text{-}6)}$ TTG in the promoters of cell cycle regulatory genes. *, the predicted

translation start is indicated by +1. (**C-F**) The promoter regions of *ntrY* (**C**), *ctrA* (**D**), *dnaA* (**E**), *gcrA* (**F**) containing at least one CAAN$_{(1\text{-}6)}$TTG motif were directly bound by the phosphorylated NtrX protein *in vitro*, as based on EMSA. His-NtrX^{D53E}, the His-NtrX fusion protein containing a substitution of D53 (phosphorylation site) to E in (**C**). Probe P*dnaA*s is the DNA probe P*dnaA* with C**AA**AACCC**TT**G replaced by C**GG**AACCC**CC**G in (**E**). D/P complex, DNA-protein complex; competitor, probe DNA without biotin labeling. The amounts of His-NtrX proteins were 3, 6 and 15 ng for each probe (2 nM). P, the putative transcriptional start site was predicted by the BDGP program. Blue bars, probes for EMSA; red bars, putative binding sites. All experiments were repeated twice.

Fig. 9. A NtrX-mediated transcriptional control system of *S. meliloti* cell cycle progression

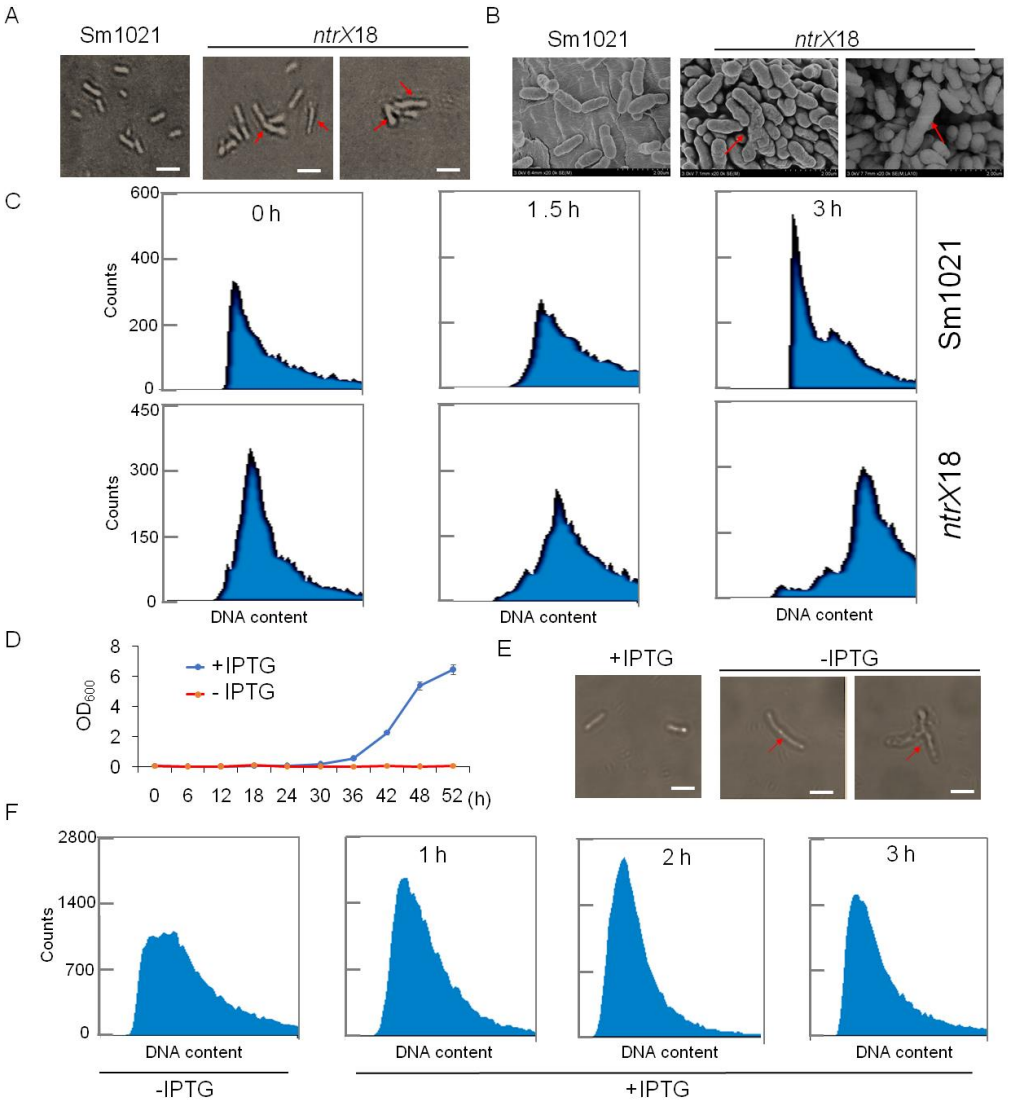

Fig.1

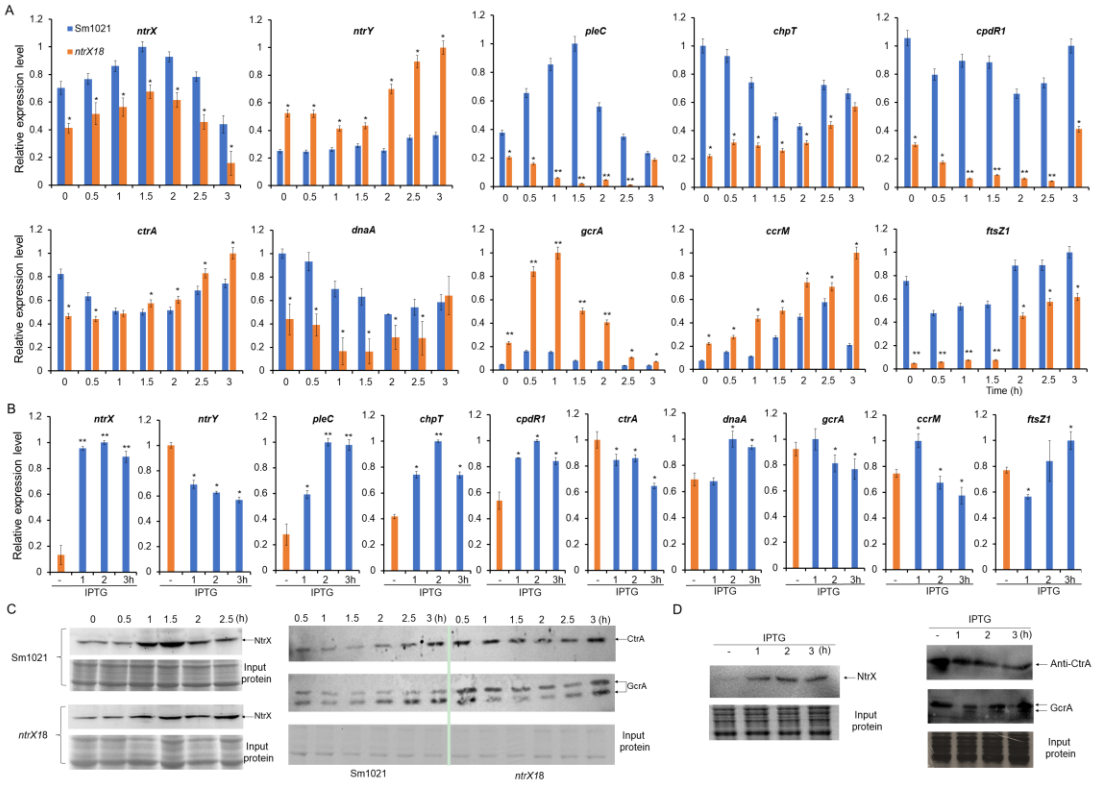

Fig.2

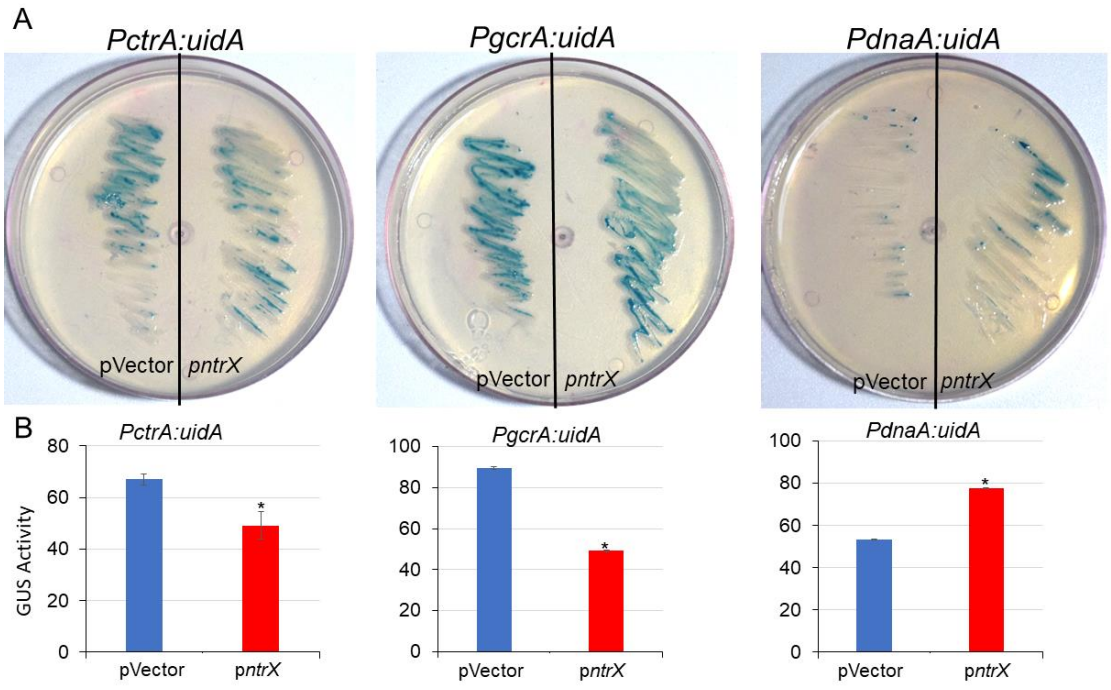

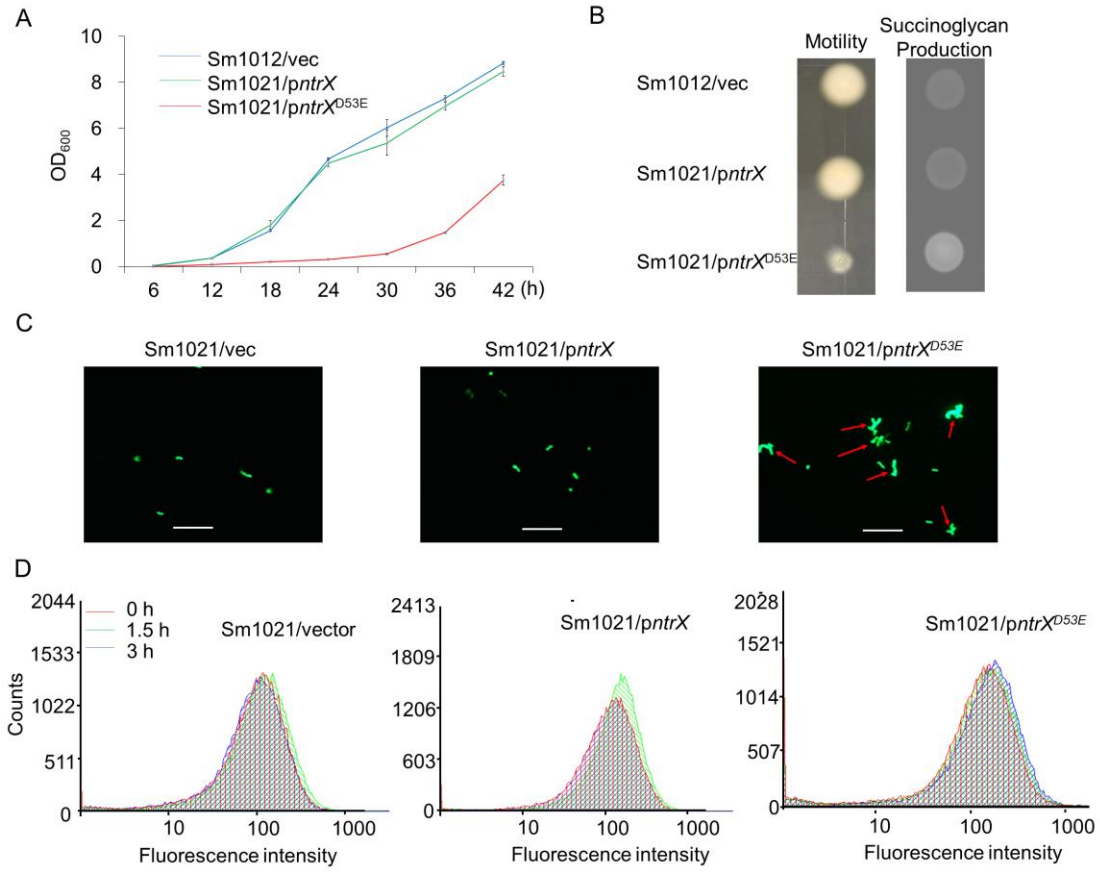

Fig. 4

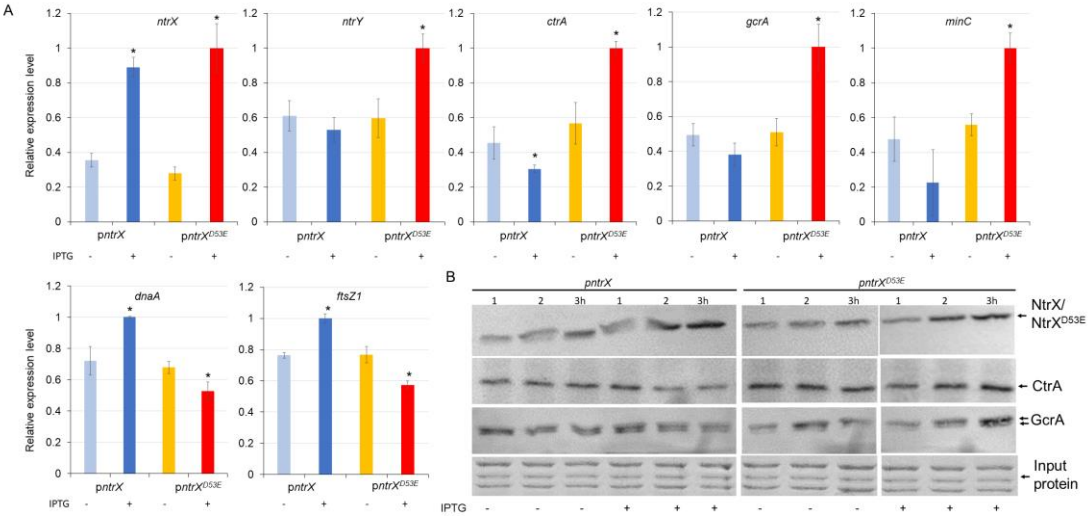

Fig. 5

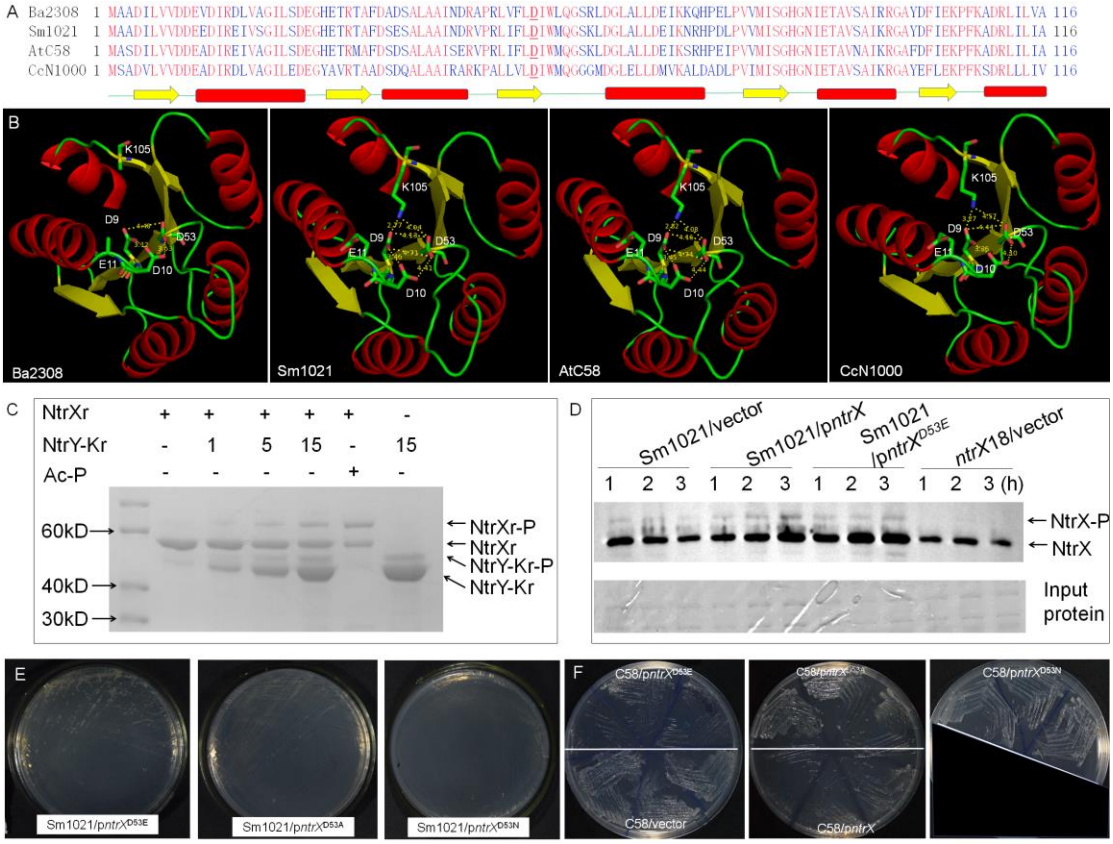

Fig. 6

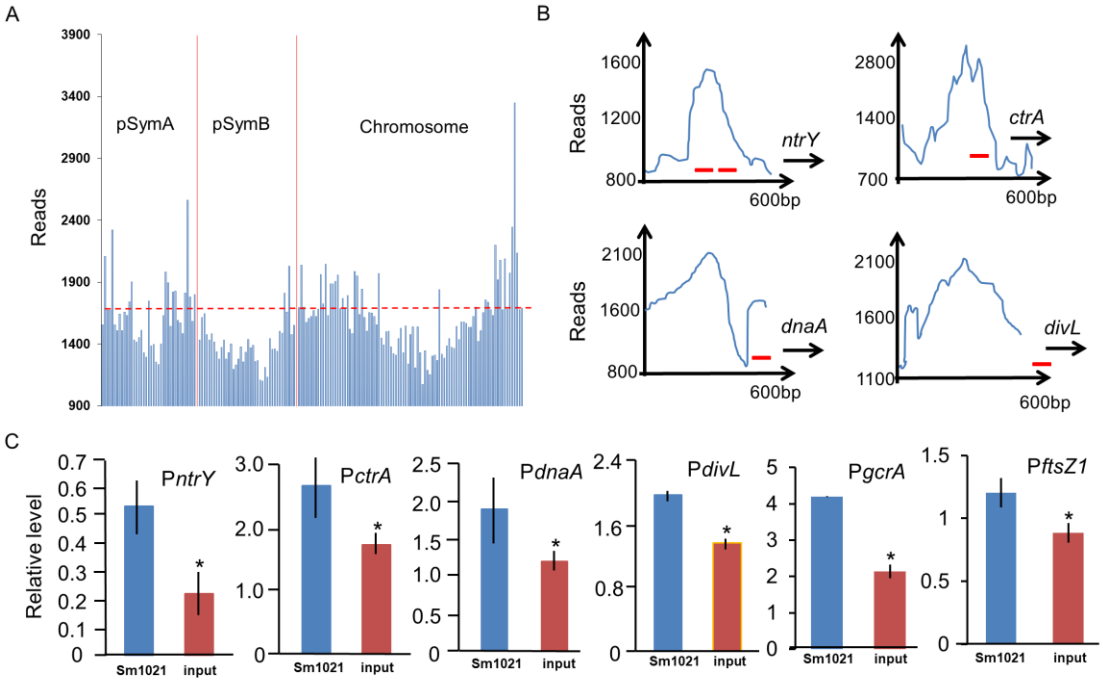

Fig. 7

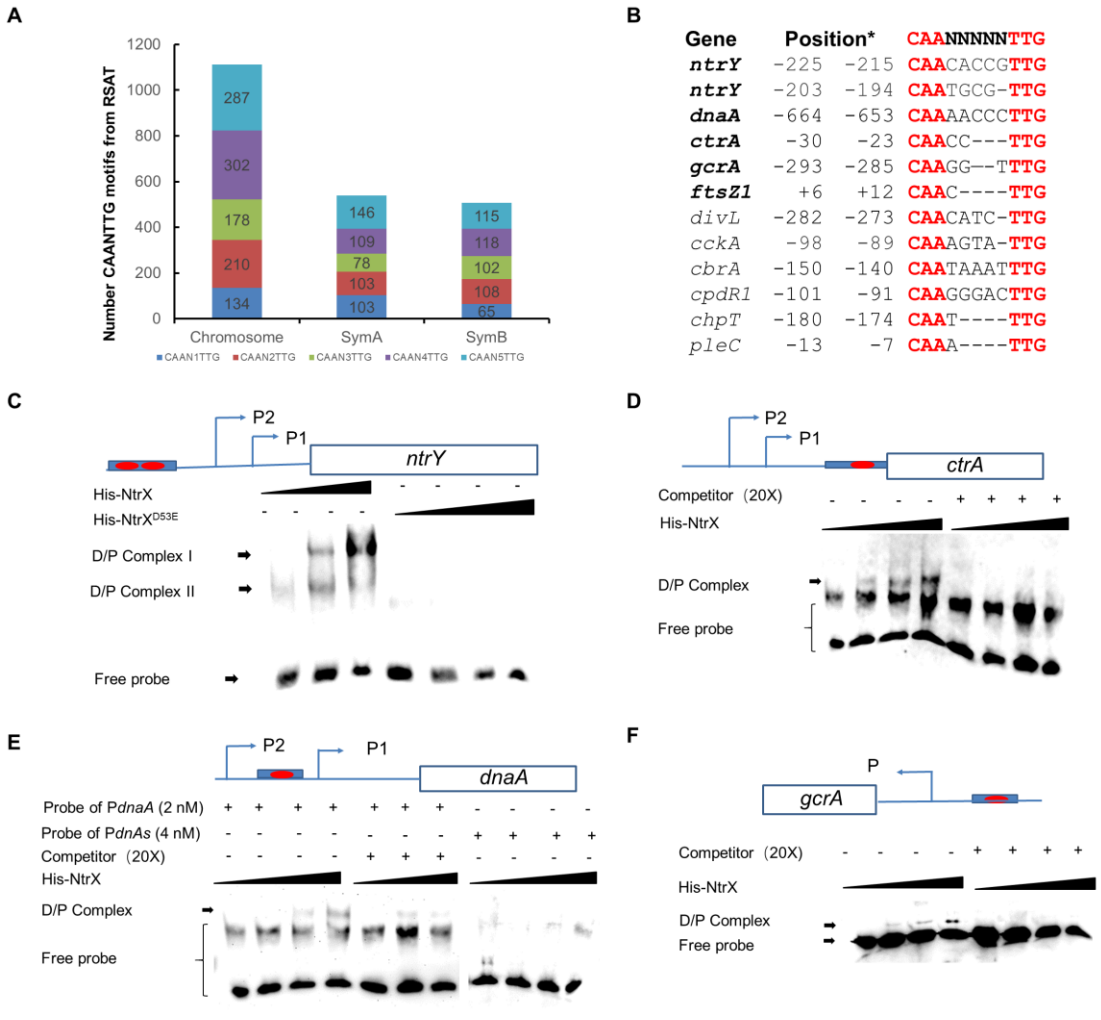

Fig. 8

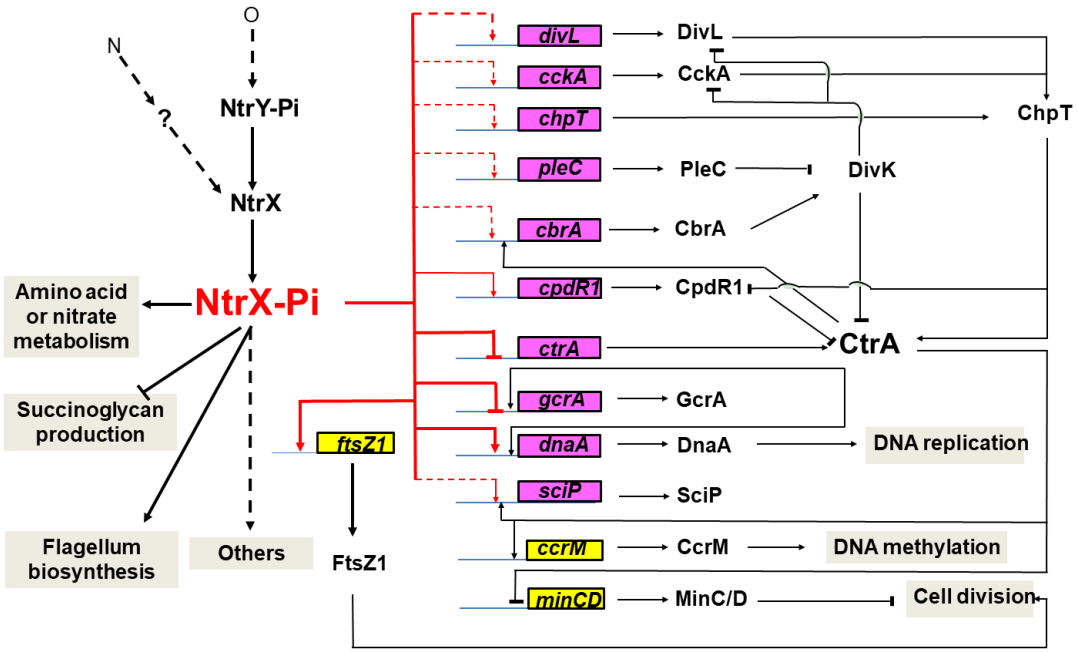

954

955 **Fig. 9**